

Title	Effect of nitridation on the growth of GaN on ZrB <sub>2</sub> (0001)/Si(111) by molecular beam epitaxy
Author(s)	Wang, Zhi-Tao; Yamada-Takamura, Y.; Fujikawa, Y.; Sakurai, T.; Xue, Q. K.
Citation	Journal of Applied Physics, 100(3): 033506-1-033506-5
Issue Date	2006-08-02
Type	Journal Article
Text version	publisher
URL	<a href="http://hdl.handle.net/10119/4516">http://hdl.handle.net/10119/4516</a>
Rights	Copyright 2006 American Institute of Physics. This article may be downloaded for personal use only. Any other use requires prior permission of the author and the American Institute of Physics. The following article appeared in Zhi-Tao Wang, Y. Yamada-Takamura, Y. Fujikawa, T. Sakurai, Q. K. Xue, J. Tolle, J. Kouvetakis, and I. S. T. Tsong, Journal of Applied Physics, 100(3), 033506 (2006) and may be found at <a href="http://link.aip.org/link/?JAPIAU/100/033506/1">http://link.aip.org/link/?JAPIAU/100/033506/1</a>
Description	

# Effect of nitridation on the growth of GaN on ZrB<sub>2</sub>(0001)/Si(111) by molecular-beam epitaxy

Zhi-Tao Wang

*Institute for Materials Research, Tohoku University, Sendai 980-8577 Japan*  
*Institute of Physics, Chinese Academy of Sciences, Beijing 100080 China*

Y. Yamada-Takamura, Y. Fujikawa, and T. Sakurai

*Institute for Materials Research, Tohoku University, Sendai 980-8577 Japan*

Q. K. Xue

*Institute of Physics, Chinese Academy of Sciences, Beijing 100080 China*

J. Tolle and J. Kouvetakis

*Department of Chemistry and Biochemistry, Arizona State University, Tempe, Arizona 85287-1604*

I. S. T. Tsong

*Department of Physics and Astronomy, Arizona State University, Tempe, Arizona 85287-1504*

(Received 11 January 2006; accepted 3 May 2006; published online 2 August 2006)

The effect of nitridation on the epitaxial growth of GaN on lattice-matched ZrB<sub>2</sub>(0001) films prepared *ex situ* and *in situ* was studied using an ultrahigh-vacuum molecular-beam epitaxy (MBE)-scanning probe microscopy system. The growth of GaN was carried out by rf-plasma-assisted MBE, and epitaxy of wurtzite GaN was observed on both *ex situ* and *in situ* prepared ZrB<sub>2</sub> samples. The polarity was found to be consistently N-polar regardless of the samples, based on the observation of a series of N-polar Ga-rich reconstructions: (3 × 3), (6 × 6), and *c*(6 × 12). The nitridation of ZrB<sub>2</sub> film was conducted by exposing it to active nitrogen and well-ordered hexagonal-BN (*h*-BN) formation was observed when the annealing temperature was above 900 °C. The partially formed BN layer affected neither the epitaxy nor the polarity of GaN, but when the surface was fully covered with well-ordered *h*-BN, GaN growth did not occur. © 2006 American Institute of Physics. [DOI: 10.1063/1.2218763]

## I. INTRODUCTION

Wurtzite gallium nitride (GaN) and related nitrides are typically grown on substrates with large lattice mismatch, such as sapphire (16%) and  $\alpha$ -SiC (4%). Although short-wavelength light-emitting diodes and laser diodes have been fabricated from these nitride films, lattice-matched substrates are desirable in terms of improved crystal growth. Recently, zirconium diboride (ZrB<sub>2</sub>) has been proposed as a lattice-matched substrate for GaN growth,<sup>1</sup> and they have been demonstrated to be viable substrates for III-nitrides.<sup>2</sup> ZrB<sub>2</sub> is a semimetal with an AlB<sub>2</sub>-type hexagonal structure, and its in-plane lattice constant of 3.168 Å matches closely to that of 3.189 Å for GaN (0.7% mismatch). Furthermore, the thermal expansion coefficient of ZrB<sub>2</sub> ( $5.9 \times 10^{-6} \text{ K}^{-1}$  along [10 $\bar{1}$ 0]) is similar to that of GaN ( $5.6 \times 10^{-6} \text{ K}^{-1}$  along [10 $\bar{1}$ 0]), which minimizes the thermal strain (5% mismatch). High thermal conductivity (100 W m<sup>-1</sup> K<sup>-1</sup> along [0001] and 140 W m<sup>-1</sup> K<sup>-1</sup> along [10 $\bar{1}$ 0]) comparable to single-crystal Si, and low electrical resistivity (4.6  $\mu\Omega$  cm) comparable to metals, are also favorable in terms of device performance and design. All of these properties of ZrB<sub>2</sub> make it a promising substrate for GaN growth.

Single-crystalline ZrB<sub>2</sub>(0001) films can be epitaxially grown on Si(111) by the thermal decomposition of unimolecular precursor Zr(BH<sub>4</sub>)<sub>4</sub>.<sup>3</sup> Therefore, any size of ZrB<sub>2</sub> film can be grown, limited only by the Si(111) wafer size. The growth of GaN (Refs. 3 and 4) and Al<sub>0.2</sub>Ga<sub>0.8</sub>N<sup>5</sup> on

ZrB<sub>2</sub>(0001)/Si(111) was conducted by rf plasma-assisted molecular-beam epitaxy (MBE),<sup>3</sup> ultrahigh-vacuum (UHV)-chemical vapor deposition,<sup>4</sup> and metalorganic chemical vapor deposition (MOCVD),<sup>5</sup> and all nitride films showed highly promising photoluminescence properties. We have also determined that the polarity of GaN, grown directly on ZrB<sub>2</sub>(0001)/Si(111) by rf plasma-assisted MBE, is N polar, and that the mono-N polarity is largely dependent on the interface structure.<sup>6</sup>

While the epitaxial growth of Al<sub>x</sub>Ga<sub>1-x</sub>N occurs readily on ZrB<sub>2</sub>(0001) by MOCVD at 1100 °C, it is known that the direct growth of GaN on ZrB<sub>2</sub>(0001) by MOCVD is problematic because of the preferential formation of a cubic ZrB<sub>x</sub>N<sub>1-x</sub> layer at high temperatures.<sup>7</sup> This ZrB<sub>x</sub>N<sub>1-x</sub> layer hinders GaN epitaxy. In this article, the effect of nitridation on the MBE growth of GaN on ZrB<sub>2</sub>(0001)/Si(111) is investigated in detail, using an MBE-scanning probe microscopy (SPM) system.

## II. EXPERIMENT

The experiments were carried out in an UHV MBE-SPM system. The system consists of an ULVAC MBE system and a JEOL JSPM4500A SPM system. The MBE system has an electron gun and a phosphor screen for reflection high-energy electron diffraction (RHEED). The SPM system is equipped with a SPECS XR-50 Al/Mg twin anode x-ray source and a PHOIBOS 100 hemispherical energy analyzer

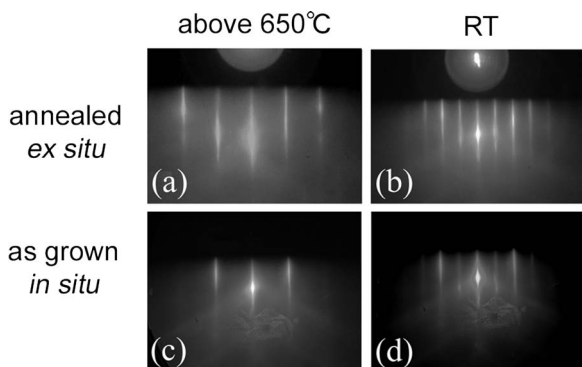


FIG. 1. RHEED patterns of (a) and (b) annealed *ex situ*-prepared  $\text{ZrB}_2(0001)/\text{Si}(111)$ , and (c) and (d) as-grown *in situ*-prepared  $\text{ZrB}_2(0001)/\text{Si}(111)$ , obtained with the electron beam parallel to  $\text{ZrB}_2(11\bar{2}0)$ . The patterns (a) and (c) were measured at a temperature higher than  $650^\circ\text{C}$ , while (b) and (d) were measured at RT.

for x-ray photoelectron spectroscopy (XPS). The base pressure of the whole system is better than  $1 \times 10^{-8}$  Pa.

The single-crystalline  $\text{ZrB}_2(0001)$  film, used as a substrate in this study, was grown *in situ* or *ex situ* by thermal decomposition of  $\text{Zr}(\text{BH}_4)_4$  under UHV on  $\text{Si}(111)$  held at  $900^\circ\text{C}$ .<sup>3</sup> The *ex situ*-grown samples were first ultrasonically cleaned with acetone, ethanol, and deionized water, and then dried by hot air—prior to loading into the MBE-SPM system via a loadlock. The samples were then annealed by direct current and the temperature was set to  $750\text{--}800^\circ\text{C}$ —measured by a pyrometer—to remove surface oxides.<sup>6</sup>

The epitaxial growth of GaN was conducted by thermally evaporated Ga and rf-nitrogen plasma. The rf-plasma source (rf-2.75, SVT Associates) was operated at a fixed condition of 300 W power with a  $\text{N}_2$  pressure of  $3 \times 10^{-3}$  Pa. The Ga effusion cell was heated to a temperature in the range of  $950\text{--}1040^\circ\text{C}$  (beam equivalent pressure:  $0.8\text{--}3.0 \times 10^{-4}$  Pa) depending on the Ga/N flux ratio required for the experiment. For the typical growth procedure, the substrate temperature was set to  $700^\circ\text{C}$ , and the nitrogen plasma was ignited shortly before opening the shutters in front of the sample and the Ga cell. The growth was monitored by RHEED using a 13 keV electron beam.

XPS spectra were measured using nonmonochromatized  $\text{Al K}\alpha$  radiation, and the size of the measured area was approximately  $700 \mu\text{m}$  in diameter. Scanning tunneling microscopy (STM) images were obtained by an electrochemically etched tungsten tip with constant tunneling current. Noncontact atomic force microscopy (NC-AFM) images were obtained by reflective metal-coated Si cantilever (Nanosensors, resonance frequency: 300 kHz, force constant: 50 N/m) with a constant frequency shift between  $-60$  and  $-90$  Hz. The cantilever was driven by constant excitation voltage, and no bias voltage was applied to the sample.

### III. RESULTS AND DISCUSSION

The annealed oxide-free  $\text{ZrB}_2$  film prepared *ex situ* and as-grown  $\text{ZrB}_2$  film prepared *in situ* displayed identical RHEED patterns as shown in Fig. 1. In both cases, a streaky  $\text{ZrB}_2(0001)\text{--}(1 \times 1)$  pattern was observed at temperatures

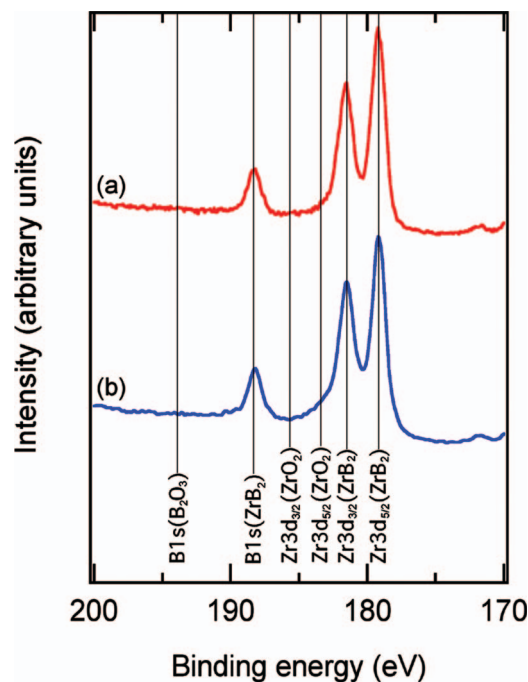


FIG. 2. (Color) XPS spectra of (a) annealed *ex situ*-prepared  $\text{ZrB}_2(0001)/\text{Si}(111)$  and (b) as grown *in situ*-prepared  $\text{ZrB}_2(0001)/\text{Si}(111)$  measured with  $\text{Al K}\alpha$  radiation. Only  $\text{ZrB}_2$ -related Zr 3d and B 1s peaks are observed.

above  $650^\circ\text{C}$ , as shown in Figs. 1(a) and 1(c). When the sample was cooled down to temperature below  $650^\circ\text{C}$ ,  $(2 \times 2)$  streaks appeared. A  $\text{ZrB}_2(0001)\text{--}(2 \times 2)$  RHEED pattern at room temperature (RT) is shown in Figs. 1(b) and 1(d). Transition between  $(1 \times 1)$  and  $(2 \times 2)$  was reversible in both samples. The XPS spectra of the annealed oxide-free *ex situ* sample and the as-grown *in situ* sample are shown in Fig. 2.  $\text{ZrB}_2$ -related peaks<sup>8</sup> at 188.3 (B 1s), 181.5 (Zr 3d<sub>3/2</sub>), and 179.2 (Zr 3d<sub>5/2</sub>) eV were observed, and impurity peaks, such as C 1s or O 1s, were not observed for both samples. The results demonstrate that the annealed *ex situ*-prepared film is as good as as-grown *in situ* prepared film, and no different result was observed between two films in the following experiments.

GaN was grown on clean  $\text{ZrB}_2(0001)\text{--}(1 \times 1)$  at  $700^\circ\text{C}$  with a slightly Ga-rich condition—identical to the one we used for direct GaN growth on  $\text{Si}(111)$ .<sup>9</sup> The evolution of the RHEED pattern during the growth is shown in Fig. 3. The electron beam was parallel to  $\text{ZrB}_2(11\bar{2}0)$ . The pattern changed from a streaky  $\text{ZrB}_2(0001)\text{--}(1 \times 1)$  pattern [Fig. 3(a)] to a spotty wurtzite GaN(0001) pattern [Fig. 3(b)] a few seconds after the shutters were opened. The spotty pattern demonstrates the three-dimensional (3D) nucleation of wurtzite GaN (Ref. 10) on  $\text{ZrB}_2$ . The diffraction pattern corresponding to zincblende GaN was not observed at the substrate temperature of  $700^\circ\text{C}$ . Mixed phase nucleation of wurtzite and zincblende GaN, followed by wurtzite phase growth, was observed when the substrate temperature was decreased to  $550\text{--}660^\circ\text{C}$  (not shown). Zincblende GaN nucleation, at a low substrate temperature and/or a high Ga flux, is previously observed for the GaN growth on sapphire by MBE.<sup>10</sup> Single-phase nucleation and growth of wurtzite

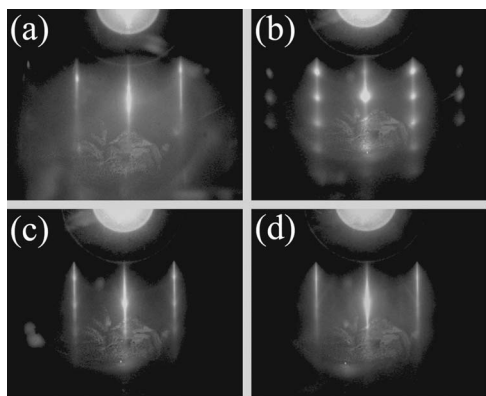


FIG. 3. RHEED pattern evolution during the growth of GaN on  $\text{ZrB}_2(0001)/\text{Si}(111)$  obtained with the electron beam parallel to  $\text{ZrB}_2\langle 11\bar{2}0 \rangle$ . (a)  $\text{ZrB}_2(0001)-(1 \times 1)$  pattern of  $\text{ZrB}_2(0001)/\text{Si}(111)$  at GaN growth temperature of  $700^\circ\text{C}$ , (b) wurtzite GaN pattern observed a few seconds after the GaN growth began, (c) wurtzite spots and  $\text{GaN}\{0001\}-(1 \times 1)$  streaks, and (d) streaky  $\text{GaN}\{0001\}-(1 \times 1)$ .

GaN on  $\text{ZrB}_2$ , observed in this study, is probably due to a higher substrate temperature and suitable Ga/N flux ratio compared to the previous studies.<sup>3,11</sup> The change in growth mode from 3D to two dimensional—most likely due to the surfactant effect of excess Ga—was observed as a decreased intensity of spots and an increased intensity of streaks in Fig. 3(c), in comparison with Fig. 3(b). After growing for 30 min, a streaky  $\text{GaN}(0001)-(1 \times 1)$  pattern without spots, shown in Fig. 3(d), was observed; demonstrating that the atomically smooth GaN surface was obtained. Based on the peak separations and rotation symmetry, the epitaxial relationship between GaN and  $\text{ZrB}_2$  was determined to be  $\text{GaN}\langle 0001 \rangle // \text{ZrB}_2\langle 0001 \rangle$  and  $\text{GaN}\langle 11\bar{2}0 \rangle // \text{ZrB}_2\langle 11\bar{2}0 \rangle$ ; reflecting their near-perfect in-plane lattice matching.

Deposition of Ga on the  $\text{GaN}(0001)-(1 \times 1)$  at RT [Fig. 4(a)] resulted in  $(3 \times 3)$ ,  $(6 \times 6)$ , and  $c(6 \times 12)$  RHEED patterns with increasing Ga coverage, as shown in Figs. 4(b)–4(d). The observed reconstructions demonstrate the N-polarity of the grown film.<sup>12</sup> Because of the insulating nature of the GaN film grown on  $\text{ZrB}_2/\text{Si}(111)$ , AFM was used to image the reconstructed surfaces instead of STM. AFM images of  $(3 \times 3)$ ,  $(6 \times 6)$ , and  $c(6 \times 12)$  were observed, as shown in Fig. 5, which correspond to the RHEED

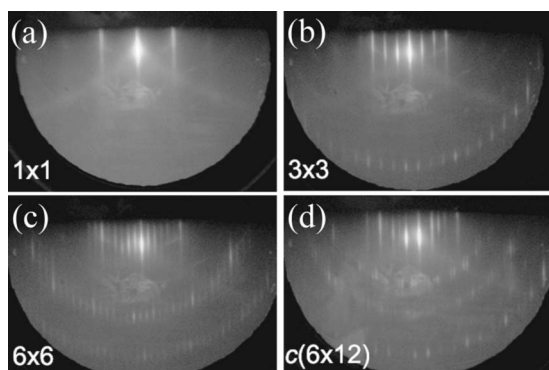


FIG. 4. RHEED patterns of (a) as-grown GaN film showing  $\text{GaN}\{0001\}-(1 \times 1)$ , and after RT deposition of Ga showing N-polarity related reconstructions: (b)  $(3 \times 3)$  (c)  $(6 \times 6)$  (d)  $c(6 \times 12)$ .

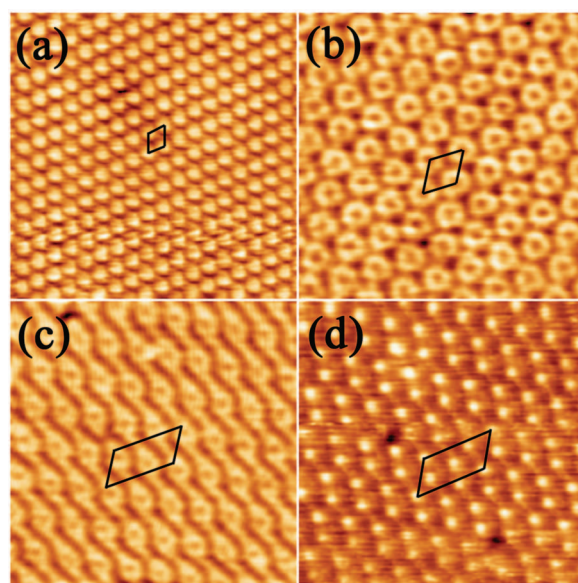


FIG. 5. (Color) High-resolution NC-AFM images ( $15 \times 15 \text{ nm}^2$ ) of GaN film grown on  $\text{ZrB}_2/\text{Si}(111)$ . Unit cells are indicated with edges along  $\langle 11\bar{2}0 \rangle$ . (a)  $(3 \times 3)$ ; (b)  $(6 \times 6)$ ; (c)  $(6 \times 12)$  observed with a (c) large frequency shift (small probe-sample distance) and a (d) small frequency shift (large probe-sample distance). Images (c) and (d) agree with filled-state and empty-state STM images (see Ref. 9). All of the reconstructions are related to  $\text{GaN}(000\bar{1})$ .

patterns. The images were nearly identical to the previously observed STM images of Ga-rich  $\text{GaN}(000\bar{1})$  surfaces.<sup>9,12</sup> Smith *et al.*<sup>12,13</sup> studied the bias voltage dependence of the STM images for each of these Ga-rich  $\text{GaN}(000\bar{1})$  reconstructions, and only observed strong dependence for the  $c(6 \times 12)$  structure. We note that the AFM images of the  $c(6 \times 12)$  structure, observed with a different frequency shift [Figs. 5(c) and 5(d)], are nearly identical to the filled- and empty-state STM images in Ref. 13 and also in our previous study.<sup>9</sup> Since optimization to achieve atomic resolution was performed by gradually increasing the frequency shift, i.e., decreasing probe-sample distance, the probe must have interacted with the empty state spreading outside of the filled state of the  $c(6 \times 12)$  structure; giving AFM images identical to the empty-state STM image at small frequency shift and the filled-state STM image at a large frequency shift. Since the  $c(6 \times 12)$  is the most Ga-rich reconstruction on a N-polar surface, it seems natural that the empty state tends to be localized at the outermost Ga. The  $\text{GaN}\{0001\}$  films grown on an *ex situ*- and *in situ*-prepared  $\text{ZrB}_2(0001)$  film showed identical Ga-rich reconstructions, and thus were determined to be N-polar—based on the Ga-rich reconstruction observed by RHEED and AFM. The film polarity was not affected by the growth conditions, and this is consistent with the result obtained in the previous theoretical study of a  $\text{GaN}(0001)/\text{ZrB}_2(0001)$  interface structure, which has shown that one nitrogen atom bonded to three zirconium atoms at the interface—between N-polar GaN and Zr-terminated  $\text{ZrB}_2$ —is the most stable interface structure throughout the considered chemical potential range.<sup>6,14</sup>

Exposure of  $\text{ZrB}_2(0001)$  to nitrogen plasma at the temperature of GaN growth, prior to GaN growth, did not

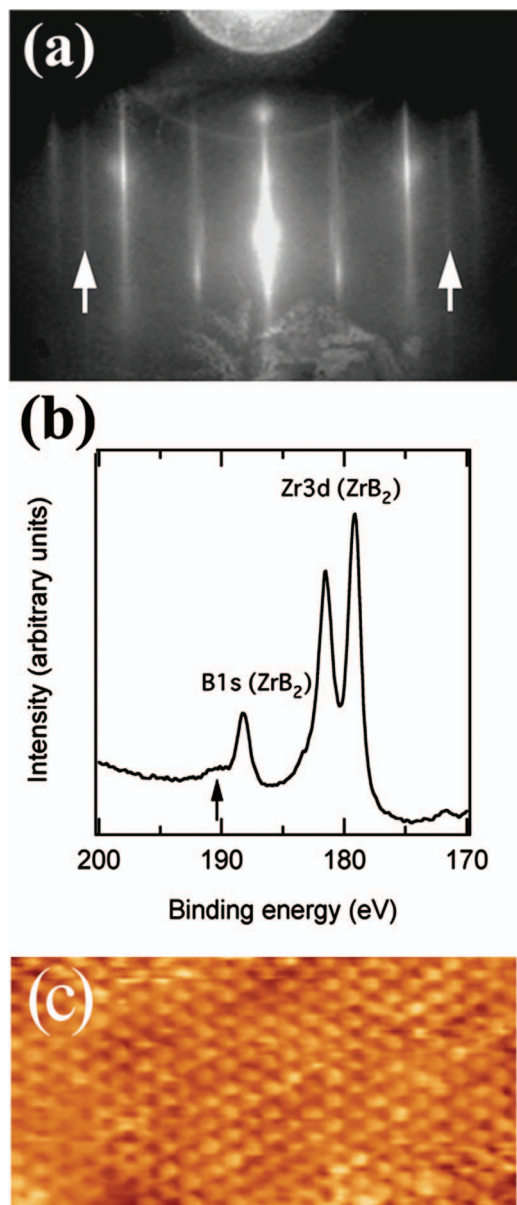


FIG. 6. (Color) Additional features observed in (a) a RHEED pattern, (b) an XPS spectrum, and (c) an STM image ( $2.5 \times 5 \text{ nm}^2$ ,  $+0.1 \text{ V}$ , and  $0.2 \text{ nA}$ ) after nitriding  $\text{ZrB}_2(0001)-(2 \times 2)$  by exposure to active nitrogen and annealing at  $900^\circ\text{C}$ . White arrows in the RHEED pattern and a black arrow in the XPS spectrum demonstrate boron nitride formation. A hexagonal structure with lattice constant corresponding to  $h\text{-BN}(0001)-(1 \times 1)$  is observed in the STM image.

change the above-mentioned growth mode or the polarity, even when the nitridation changed the streaky  $\text{ZrB}_2(0001)-(1 \times 1)$  pattern into an amorphous pattern. Epitaxial nucleation and an atomically smooth surface, which shows N-polar-related Ga-rich reconstruction upon the additional Ga deposition, was reproducibly observed. The result is similar to the case of direct GaN growth on nitridated Si(111), where GaN grows epitaxially on the nitridated Si(111) surface giving amorphous RHEED pattern.<sup>9</sup>

When the sample was exposed to active nitrogen at a temperature above  $900^\circ\text{C}$ , or annealed after exposure to active nitrogen at a temperature above  $900^\circ\text{C}$ , additional streaks were observed in the RHEED pattern [Fig. 6(a)]. This

demonstrates the formation of a well-ordered structure with periodicity of  $2.16 \pm 0.02 \text{ \AA}$ , measured with  $\text{ZrB}_2(0001)-(1 \times 1)$  as a reference. This corresponds well with a hexagonal-BN ( $h\text{-BN}$ )  $(0001)-(1 \times 1)$  pattern with the electron beam parallel to  $h\text{-BN}\langle 11\bar{2}0 \rangle$  ( $2.18 \text{ \AA}$ ). In the XPS spectra, an additional peak was observed, close to  $\text{ZrB}_2$ -related B 1s peak, as shown in Fig. 6(b). The additional peak corresponds well with BN-related B 1s peak position, while Zr 3d peaks showed no change before and after nitridation. The hexagonal structure with a lattice constant of  $2.4 \pm 0.2 \text{ \AA}$ , which corresponds well with  $h\text{-BN}(0001)-(1 \times 1)$  ( $a$ -lattice constant:  $2.51 \text{ \AA}$ ), was also observed by STM, as shown in Fig. 6(c). The results demonstrate the formation of  $h\text{-BN}$  upon high-temperature nitridation of  $\text{ZrB}_2$  with  $h\text{-BN}(0001)//\text{ZrB}_2\langle 0001 \rangle$  and  $h\text{-BN}\langle 11\bar{2}0 \rangle//\text{ZrB}_2\langle 11\bar{2}0 \rangle$ .

By STM observations, it was possible to examine how much of the surface was covered with nitride. The  $\text{ZrB}_2(0001)-(2 \times 2)$  area coexisted with the  $h\text{-BN}(0001)-(1 \times 1)$  area depending on the exposure time and annealing temperature. The polarity of GaN grown on nitridated  $\text{ZrB}_2$  with the two coexisting structures was N polar, while GaN nucleation was not observed on  $\text{ZrB}_2$  fully covered with  $h\text{-BN}$ . The high inertness of the graphitic BN layer seems to prohibit GaN nucleation. When the coexisting  $\text{ZrB}_2(0001)-(2 \times 2)$  area was present, GaN growth was most likely achieved through nucleation on the  $\text{ZrB}_2(0001)-(2 \times 2)$  area followed by lateral overgrowth on the  $h\text{-BN}(0001)-(1 \times 1)$  area. Applying the epitaxial lateral overgrowth (ELO) method<sup>15</sup> to elemental-source GaN-MBE growth is known to be difficult because of GaN nucleation on dielectric layers.<sup>16</sup> Since  $h\text{-BN}$  effectively prevents GaN nucleation, patterning of  $\text{ZrB}_2$  through selective nitridation may provide a way to grow GaN with less defects through ELO.

#### IV. CONCLUSIONS

We have demonstrated that an oxide-free and well-defined  $\text{ZrB}_2(0001)$  surface, as good as the surface of an as-grown  $\text{ZrB}_2(0001)$  film, can be prepared by annealing *ex situ*-prepared  $\text{ZrB}_2(0001)/\text{Si}(111)$  in a UHV. The polarity of GaN grown on the  $\text{ZrB}_2$  films was studied by the observation of a series of Ga-rich reconstructions using RHEED and NC-AFM, and it was determined to be consistently N-polar regardless of growth conditions and whether the  $\text{ZrB}_2$  films were prepared *ex situ* or *in situ*. This is consistent with the previous theoretical study.<sup>6,14</sup> When  $\text{ZrB}_2(0001)$  was nitridated at a temperature above  $900^\circ\text{C}$ ,  $h\text{-BN}$  was formed, and high GaN nucleation selectivity was observed between clean and  $h\text{-BN}$ -covered  $\text{ZrB}_2$ . This study demonstrates the significance of understanding surface and interface properties in order to obtain better control of polar film nucleation and growth.

#### ACKNOWLEDGMENT

Three of the authors (J. T., J. K., and I. S. T. T.) acknowledge support from the National Science Foundation (Grant Nos. DMR-0221993 and DMR-0303237).

- <sup>1</sup>H. Kinoshita, S. Otani, S. Kamiyama, H. Amano, I. Akasaki, J. Suda, and H. Matsunami, *Jpn. J. Appl. Phys., Part 2* **40**, L1280 (2001); **42**, 2260 (2003).
- <sup>2</sup>J. Suda and H. Matsunami, *J. Cryst. Growth* **237**, 1114 (2002); S. Kamiyama, S. Takanami, Y. Tomida, K. Iida, T. Kawashima, S. Fukui, M. Iwaya, H. Kinoshita, T. Matsuda, T. Yasuda, S. Otani, H. Amano, and I. Akasaki, *Phys. Status Solidi A* **200**, 67 (2003).
- <sup>3</sup>J. Tolle, R. Roucka, C. Ritter, P. A. Crozier, A. V. G. Chizmeshya, I. S. T. Tsong, and J. Kouvetakis, *Appl. Phys. Lett.* **82**, 2398 (2003).
- <sup>4</sup>R. A. Trivedi, J. Tolle, A. V. G. Chizmeshya, R. Roucka, C. Ritter, J. Kouvetakis, and I. S. T. Tsong, *Appl. Phys. Lett.* **87**, 072107 (2005).
- <sup>5</sup>J. Tolle, J. Kouvetakis, D.-W. Kim, S. Mahajan, A. Bell, F. A. Ponce, I. S. T. Tsong, M. L. Kottke, and Z. D. Chen, *Appl. Phys. Lett.* **84**, 3510 (2004).
- <sup>6</sup>Y. Yamada-Takamura, Z. T. Wang, Y. Fujikawa, T. Sakurai, Q. K. Xue, J. Tolle, P.-L. Liu, A. V. G. Chizmeshya, J. Kouvetakis, and I. S. T. Tsong, *Phys. Rev. Lett.* **95**, 266105 (2005).
- <sup>7</sup>Y. Tomida, S. Nitta, S. Kamiyama, H. Amano, I. Akasaki, S. Otani, H. Kinoshita, R. Liu, A. Bell, and F. A. Ponce, *Appl. Surf. Sci.* **216**, 502 (2003).
- <sup>8</sup>R. Singh, M. Trenary, and Y. Paderno, *Surf. Sci. Spectra* **7**, 310 (2000).
- <sup>9</sup>Z. T. Wang, Y. Yamada-Takamura, Y. Fujikawa, T. Sakurai, and Q. K. Xue, *Appl. Phys. Lett.* **87**, 032110 (2005).
- <sup>10</sup>H. Okumura, K. Balakrishnan, H. Hamaguchi, T. Koizumi, S. Chichibu, H. Nakanishi, T. Nagatomo, and S. Yoshida, *J. Cryst. Growth* **189**, 364 (1998).
- <sup>11</sup>R. Armitage, K. Nishizono, J. Suda, and T. Kimoto, *J. Cryst. Growth* **284**, 369 (2005).
- <sup>12</sup>A. R. Smith, R. M. Feenstra, D. W. Greve, J. Neugebauer, and J. E. Northrup, *Phys. Rev. Lett.* **79**, 3934 (1997).
- <sup>13</sup>A. R. Smith, R. M. Feenstra, D. W. Greve, J. Neugebauer, and J. E. Northrup, *Appl. Phys. A: Mater. Sci. Process.* **66**, 8947 (1998).
- <sup>14</sup>P.-L. Liu, A. V. G. Chizmeshya, J. Kouvetakis, and I. S. T. Tsong, *Phys. Rev. B* **72**, 245335 (2005).
- <sup>15</sup>O. H. Nam, M. D. Bremser, T. S. Zheleva, and R. F. Davis, *Appl. Phys. Lett.* **71**, 2638 (1997).
- <sup>16</sup>J. T. Torvik, J. I. Pankove, E. Iliopoulos, H. M. Ng, and T. Moustakas, *Appl. Phys. Lett.* **72**, 244 (1998).